THE ROYAL SOCIETY

p-nitrophenyl nitronyl nitroxide: the first organic ferromagnet

By Minoru Kinoshita

Faculty of Science and Engineering, Science University of Tokyo, Daigaku-dori 1-1-1, Onoda-shi, Yamaguchi 756-0884, Japan

The transition to ferromagnetic order was realized in 1991 with the discovery of a *p*-nitrophenyl nitronyl nitroxide ($C_{13}H_{16}N_3O_4$) crystal. This was the first example of a ferromagnet without metal elements. Its ferromagnetism below the transition temperature of 0.6 K has been established by various experiments such as susceptibility, magnetization, heat capacity, zero-field muon spin rotation, neutron diffraction and ferromagnetic resonance measurements. Details of the results of these experiments are described in this paper.

Keywords: *p*-nitrophenyl nitronyl nitroxide; *p*-NPNN; muon spin rotation; pressure effect on ferromagnetism; ferromagnetic to antiferromagnetic transition; charge-transfer mechanism

1. Introduction

Solid-state properties of organic compounds have been extensively studied for several decades and it has been revealed that organic solids possess the potential ability to exhibit various interesting properties. The development of organic conductors and superconductors is one such example. In contrast to these advances, the absence of an organic ferromagnet was one of the most conspicuous problems about 10 years ago. The first explicit theoretical approach for an organic ferromagnet was proposed as early as 1963 by McConnell (1963). However, no purely organic crystal was found to be a three-dimensional 'bulk' ferromagnet, even after extensive studies on the magnetic properties of organic solids.

About 15 years ago, only a few organic radical crystals were known to exhibit an intermolecular ferromagnetic interaction. One of them was the galvinoxyl radical (Mukai *et al*. 1967; Mukai 1969). We then initiated extensive studies on this compound to search for conditions favouring the ferromagnetic interaction in organic solids. After experimental and theoretical studies over a couple of years, we derived the following conclusion (Awaga *et al*. 1986*a*–*c*, 1987*a*, *b*, 1988; Hosokoshi *et al*. 1997; Kinoshita 1991, 1993*a*). The requirement for the ferromagnetic intermolecular interaction is twofold, namely:

(a) large spin polarization within a radical molecule; and

(b) small SOMO–SOMO overlap and large SOMO–FOMO overlap between neighbouring radicals.

Here SOMO stands for the singly occupied molecular orbital, and FOMO the fully occupied (or unoccupied) molecular orbitals. Condition (a) states the requirement a radical molecule has to fulfil. The concept of spin polarization was well studied in the 1960s, particularly in odd-alternate organic compounds such as galvinoxyl and nitronyl nitroxide radicals. The spin polarization originates from an exchange interaction in a radical molecule. On the other hand, condition (b) is related to intermolecular interactions and to the relative location of the neighbouring radicals in a crystal. According to these conditions, the ferromagnetic intermolecular interaction originates in the exchange interaction within a molecule, which is always ferromagnetic. If the latter interaction is strong enough, it spreads out over a crystal through intermolecular charge-transfer interaction between SOMOs and FOMOs. The first radical employed fulfilling these conditions was *p*-nitrophenyl nitronyl nitroxide and it became the first example of an organic ferromagnet (Tamura *et al*. 1991; Nakazawa *et al*. 1992; Kinoshita 1993*b*, 1995, 1996).

2. Molecular and electronic structure of *p*-nitrophenyl nitronyl nitroxide

Figure 1*a* shows the molecular structure of *p*-nitrophenyl nitronyl nitroxide (abbreviated as *p*-NPNN hereafter). The dot near the NO group denotes the unpaired electron that is responsible for the magnetism. The unpaired electron is mobile over the whole molecule, but mostly localizes on the ONCNO moiety and resides to a very small extent on the other parts of the molecule. The highly localized nature of the unpaired electron on the ONCNO moiety assures the molecule of large spin polarization as a result of strong exchange interactions between the unpaired electron and the lone-pair electrons on the hetero atoms. This qualitative prediction is also supported by an unrestricted Hartree–Fock (UHF) calculation of the molecular orbitals. As shown in figure 1*b*, the energy of the molecular orbital containing the unpaired electron is much more stabilized than that of the fourth FOMO containing an electron of the opposite spin direction.

3. Crystal structure and magnetic interactions

There are four polymorphic forms, α-, β-, γ- and δ-phases, known for *p*-NPNN (Allemand *et al*. 1991†; Awaga *et al*. 1989*a*; Turek *et al*. 1991). The crystallographic data of these phases are summarized in table 1. Among them the orthorhombic β-phase is most stable, and the other phases gradually transform into the β-phase when maintained around room temperature. The molecular arrangement on the *ac*-plane of the β-phase crystal is shown in figure 2*a*. The molecules on the *ac*-plane are arranged in a parallel manner with the long molecular axis along the *a*-axis. Since the crystal belongs to the $F2dd$ space group, the lattice can be divided into two face-centred orthorhombic sublattices, each deviating by $\frac{1}{4}a$, $\frac{1}{4}b$ and $\frac{1}{4}c$. Thus the crystal structure is similar to that of diamond or, more precisely, zincblende, as shown schematically in figure 2*b*, where the radical is denoted by an ellipsoid. All the molecules on the *ac*-plane at $y = 0$ are tilted in one way and those at $y = \frac{1}{4}b$ are tilted in the other way with respect to the *ac*-plane. The best-fit planes of the ONCNO moiety are tilted by

† The δ-phase was initially denoted as the β_{h}-phase in this article. However, it was renamed with permission from Wudl, because its crystal structure is closely related to that of the β- and γ-phases.

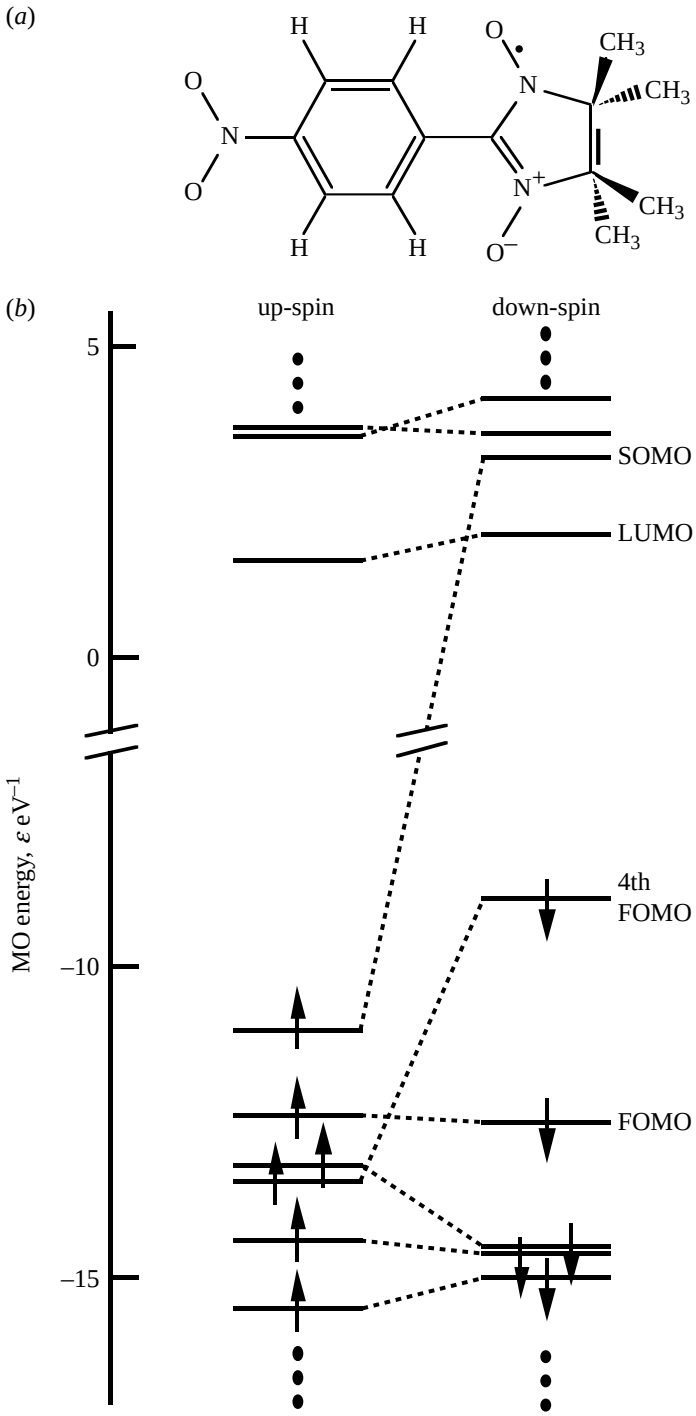

Figure 1. (*a*) Molecular formula and (*b*) molecular orbital energy levels of *p*-nitrophenyl nitronyl nitroxide. The energy levels near the singly occupied orbital (SOMO) are shown.

Table 1. *Crystal structures of p-nitrophenyl nitronyl nitroxide*

	α-phase	β-phase	γ-phase	δ-phase
system	monoclinic	orthorhombic	triclinic	monoclinic
space group	$P2_1/c$	$F2dd$	$P\bar{1}$	$P2_1/c$
a (Å)	7.302	12.347	9.193	8.963
b (Å)	7.617	19.350	12.105	23.804
c (Å)	24.677	10.960	6.471	6.728
α (deg)			97.35	
β (deg)	93.62		104.44	104.25
γ (deg)			82.22	
Z	4	8	2	4
V (Å^3)	1369.7	2618.5	687.6	1391.3
density, ρ (g cm^{-3})	1.354	1.416	1.349	1.333

$\pm 18.40°$ from the ac-plane, those of the phenyl rings by $\pm 68.45°$, and those of the nitro groups by $\pm 84.70°$.

The crystal structure at 6 K is also known from the neutron diffraction measurements (Zheludev *et al*. 1994*b*). The crystal contracts thermally maintaining its crystal symmetry, and the lattice constants of $a = 12.16$, $b = 19.01$ and $c = 10.71$ Å are reported. The contraction is largest along the c-axis (2.24%). As a result, the molecules are tilted at a greater angle than at room temperature. The tilt angles are $\pm 21.7°$, $\pm 71.2°$ and $\pm 89.1°$, respectively. These tilt angles are summarized in figure 2*c*. These changes in the tilt angle indicate that the molecules, when the crystal is cooled to 6 K, undergo librational rotation by $\pm 3.3°$ about the a-axis in preservation of the molecular shape, only the nitro groups being further rotated internally by $\pm 1°$.

It is to be noted that the density of the β-phase crystal is, as shown in table 1, the largest of the four polymorphic phases. The density increases to $\rho_c = 1.498$ g cm^{-3} at 6 K.

The expected dominant exchange paths, J_{12}, J_{13} and J_{14}, are also shown in figure 2*b* by the broken, full and dotted lines, respectively. Theoretical calculation indicates that the first two paths are ferromagnetic and the third is slightly antiferromagnetic (Okumura *et al*. 1993).

4. Ferromagnetic interactions

The paramagnetic susceptibility of the β-phase crystal was first measured in 1989 (Awaga & Maruyama 1989). The temperature dependence of magnetic susceptibility is shown in figure 3 for the field direction along the b-axis. The low field susceptibility obeys the Curie–Weiss law ($\chi = C/(T - \Theta)$) with a Weiss constant of $\Theta = +1$ K in the temperature range above *ca*. 4 K, suggesting the presence of weak ferromagnetic intermolecular interactions. Since the Weiss constant is very small, the ferromagnetic interaction is checked by measuring the field dependence of the magnetization at low temperatures. As shown in figure 4, the magnetization grows more steeply at lower temperature (Tamura *et al*. 1991). This indicates that the spins are connected by means of ferromagnetic interaction. In addition, this experiment ensures that the sample is not contaminated with a ferromagnetic impurity.

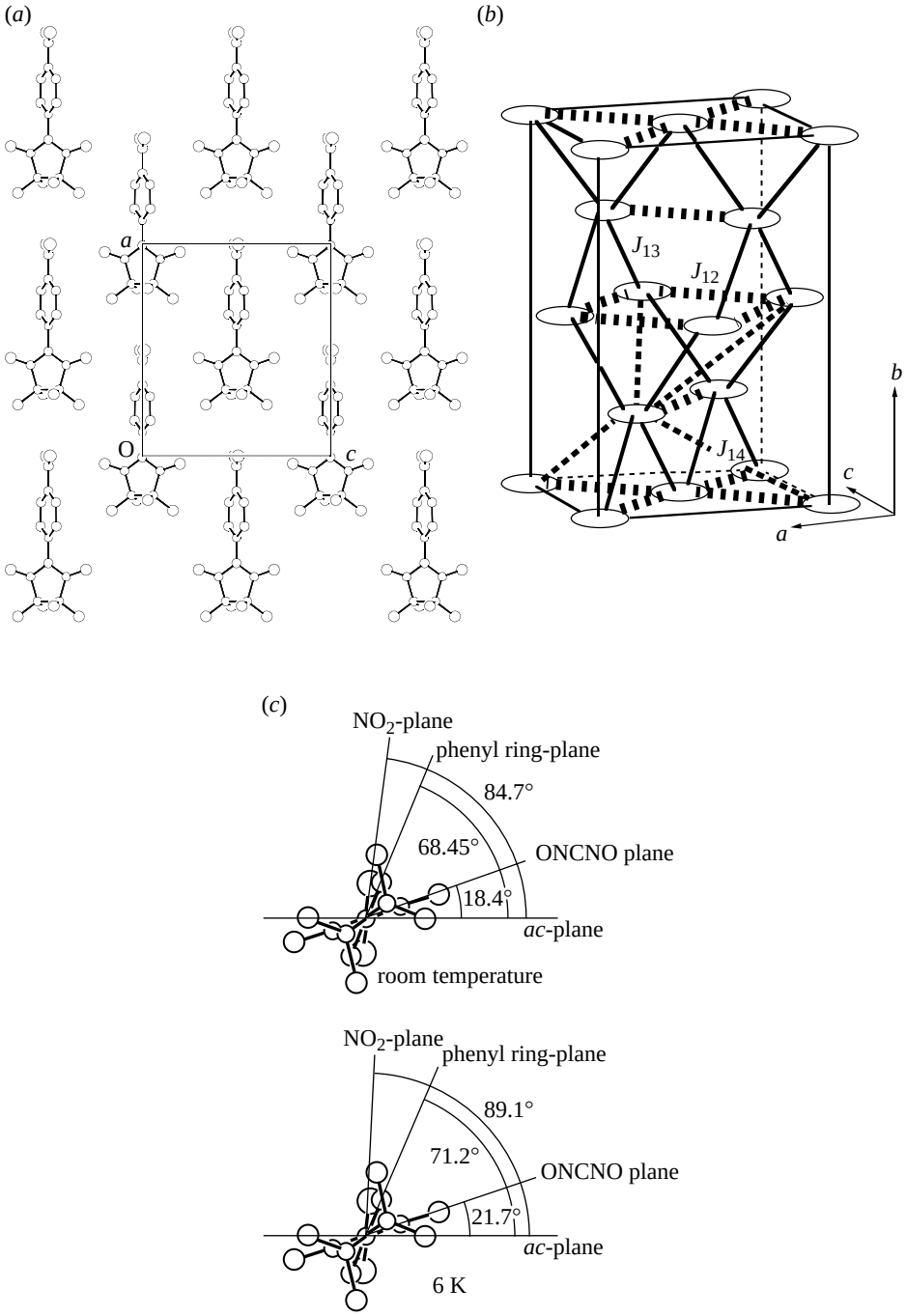

Figure 2. (*a*) The molecular arrangement on the *ac*-plane in the β-phase crystal of *p*-nitrophenyl nitronyl nitroxide. (*b*) A schematic bird's-eye-view of the crystal structure of the β-phase crystal. Each radical molecule is given by the ellipsoid. (*c*) The molecular shape viewed along the long axis at room temperature and at 6 K. The tilt angles of the best fit planes are noted with respect to the *ac*-plane.

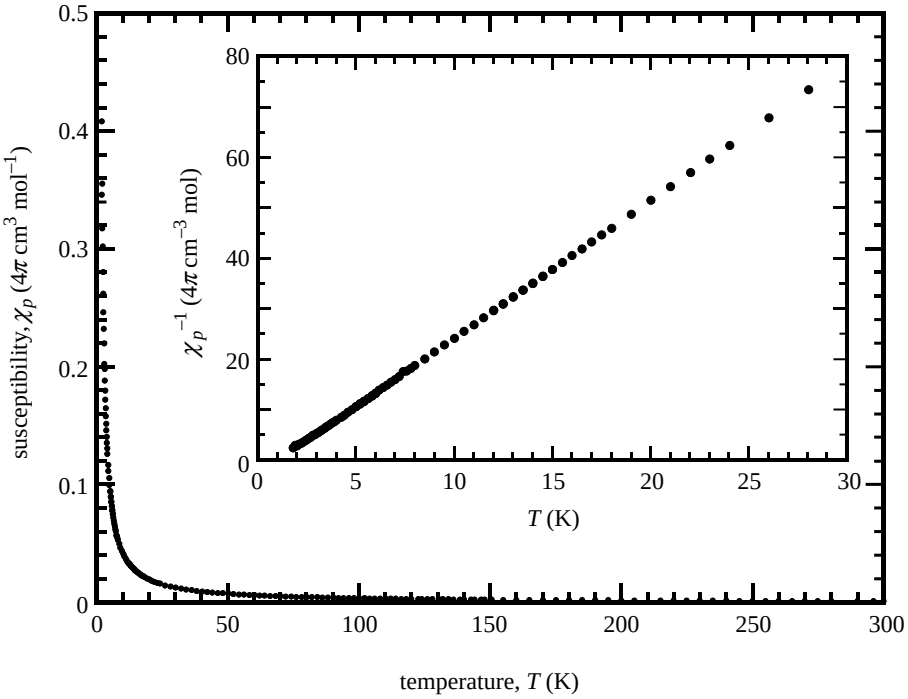

Figure 3. The temperature dependence of the static susceptibility of the β-phase p-nitrophenyl nitronyl nitroxide. The inset is the plot of reciprocal susceptibility against temperature.

5. Transition to the ferromagnetic ordered state

In 1991, the transition towards the ferromagnetic ordered state was discovered in a β-phase crystal by the measurements of AC susceptibility and heat capacity (Tamura *et al*. 1991; Nakazawa *et al*. 1992). The results of these measurements are shown in figure 5. The heat capacity has a λ-type sharp peak at the critical temperature of $T_c = 0.60$ K and reveals the existence of a transition. The corresponding entropy amounts to 85% of $R \ln 2$ in the range up to 2 K, and the transition is magnetic and bulk in nature.

As the AC susceptibility diverges at around T_c, the ordered state is, without doubt, a ferromagnetic state. In fact, the magnetization curve at 0.44 K traces a hysteresis loop characteristic of ferromagnetism, as shown in figure 6. The magnetization is almost saturated at an applied field as low as *ca.* 5 mT and the coercive force is quite small. The rapid saturation suggests a small magnetic anisotropy in the system. The g-factors observed in the paramagnetic resonance experiments are $g_a = 2.0070$, $g_b = 2.0030$ and $g_c = 2.0106$. The linewidth is also almost independent of field direction at room temperature.

6. Evidence for ferromagnetism

Further evidence for ferromagnetism has been provided by various experiments such as the measurements of the temperature dependence of heat capacity in applied magnetic fields of various strengths (Nakazawa *et al*. 1992), the zero-field muon spin

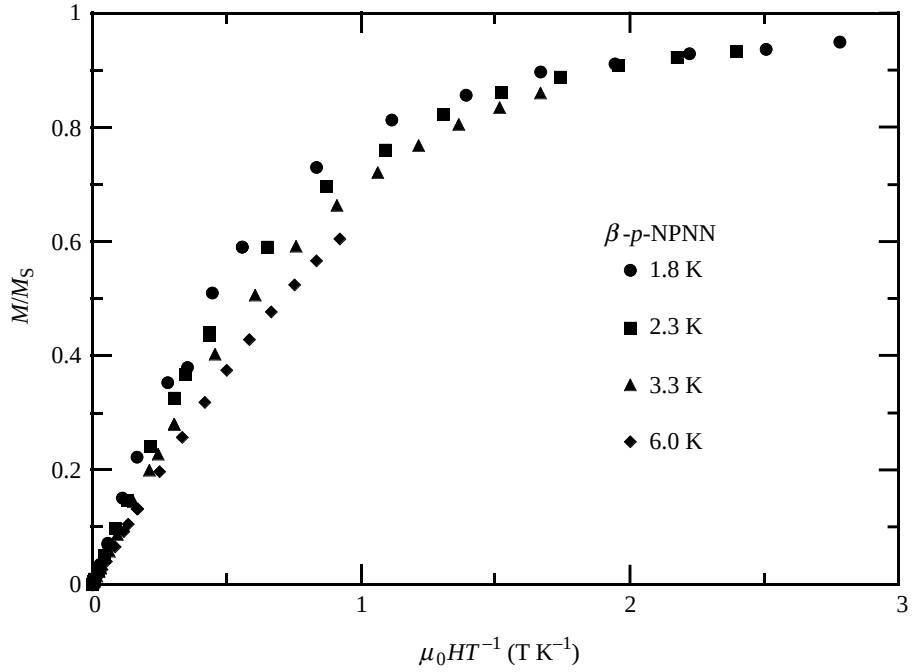

Figure 4. The plots of the magnetization of β-phase *p*-NPNN against $\mu_0 H/T$ measured at $T = 1.8$, 2.3, 3.3 and 6.0 K.

rotation (Uemura *et al*. 1993; Le *et al*. 1993; Blundell *et al*. 1995), the ferromagnetic resonance (Oshima *et al*. 1995*a*, *b*), the neutron diffraction (Zheludev *et al*. 1994*a*, *b*) and the pressure effect on the magnetic properties (Takeda *et al*. 1995, 1996; Mito *et al*. 1997).

(*a*) *Heat capacity in a magnetic field*

The heat-capacity temperature dependences at various magnetic field strengths are illustrated in figure 7 (Nakazawa *et al*. 1992). The sharp peak in the zero field is slightly rounded, and is shifted to the higher-temperature side as the magnetic field is increased. This is a feature of ferromagnetic materials. For ferromagnetic substances, the critical temperature cannot be defined in a finite magnetic field. When there is a ferromagnetic interaction among the spins, they have a tendency to align themselves in parallel along the magnetic field at very low temperatures and the spin system is ordered by a weak field slightly above the ferromagnetic transition temperature. Thus the sharp peak of the heat capacity shifts and becomes rounded as in the paramagnetic region. In the case of antiferromagnetic order, the peak remains, up to a certain field strength. Therefore, this experiment ensures the ferromagnetism of the β-phase crystal below 0.6 K.

(*b*) *Zero-field muon spin rotation*

Another piece of evidence for ferromagnetism was obtained by the measurements of zero-field muon spin rotation (ZF-μSR). Figure 8 shows some of the results of ZF-μSR experiments performed with the initial muon spin polarization perpendicular to

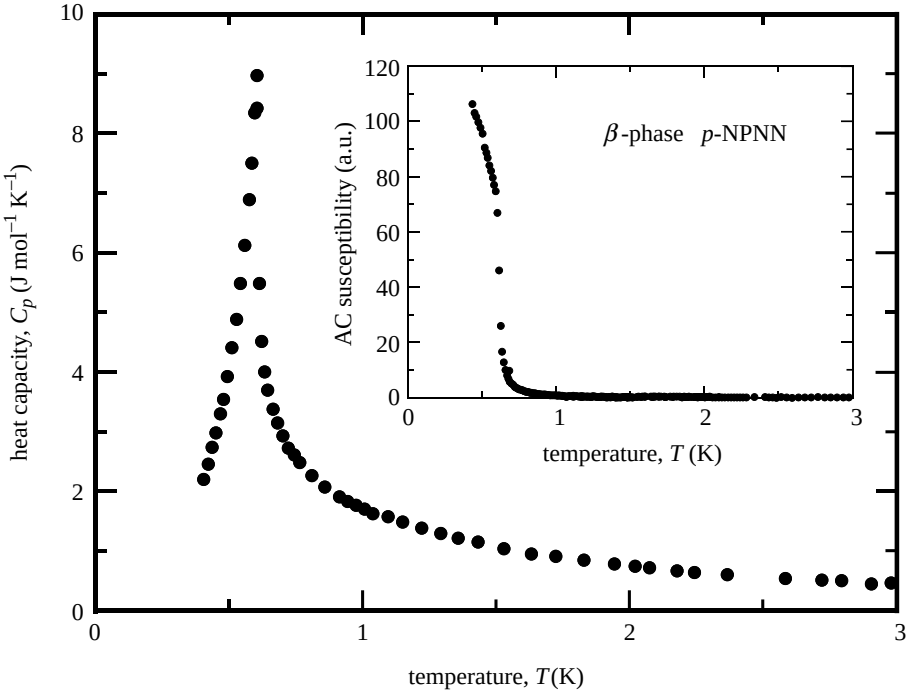

Figure 5. Temperature dependence of the magnetic heat capacity of the β-phase p-NPNN. The inset shows the temperature dependence of the AC susceptibility.

the b-axis (Uemura *et al*. 1993; Le *et al*. 1993). The oscillating signals observed at lower temperatures are due to the precession of the muons implanted in the crystal. Since there is no applied field, it is obvious that the precession is caused by the internal field coming from the spontaneous magnetization. The long-lasting oscillations indicate that the muons experience a rather homogeneous local field, which requires the ferromagnetic spin network to be commensurate with the crystallographic structure. Thus, the results of ZF-μSR experiments clearly demonstrate the appearance of spontaneous magnetic order in the β-phase crystal.

The oscillation frequency is approximately related to the internal field by $\nu_\mu = (\gamma_\mu/2\pi)B_{\rm int}$, where the muon gyromagnetic ratio $\gamma_\mu/2\pi = 135.53\,{\rm MHz\,T^{-1}}$. In figure 9, the frequency is plotted against temperature. The frequency extrapolated to 0 K corresponds approximately to the local field of 15.5 mT. The solid line in figure 9 shows a fit of $M(T) \propto M(0)[1-(T/T_{\rm c})^{\alpha}]^{\beta}$ with $\alpha = 1.86$ and $\beta = 0.32$ ($\alpha = 1.74$ and $\beta = 0.36$ are reported by Blundell *et al*. (1995)). The agreement between the μSR results and the solid line is remarkably good, which allows us to discuss the results in two interesting regions, namely $T \rightarrow 0\,{\rm K}$ and $T \rightarrow T_{\rm c}$. At temperatures well below $T_{\rm c}$, M decreases with increasing temperature as $[M(0) - M(T)] \propto T^{\alpha}$, close to the magnon-like behaviour of $[M(0) - M(T)] \propto T^{1.5}$. Near $T_{\rm c}$, $M(T) \propto (T_{\rm c} - T)^{\beta}$ with the critical magnetization exponent $\beta = 0.32$, in agreement with a value of $\frac{1}{3}$ expected for a three-dimensional Heisenberg system. The temperature dependence of $M(T)$ in p-NPNN is thus consistent with that of three-dimensional Heisenberg systems both at low temperature and near $T_{\rm c}$.

The amplitude of the oscillations diminishes to *ca.* 20% when the initial muon

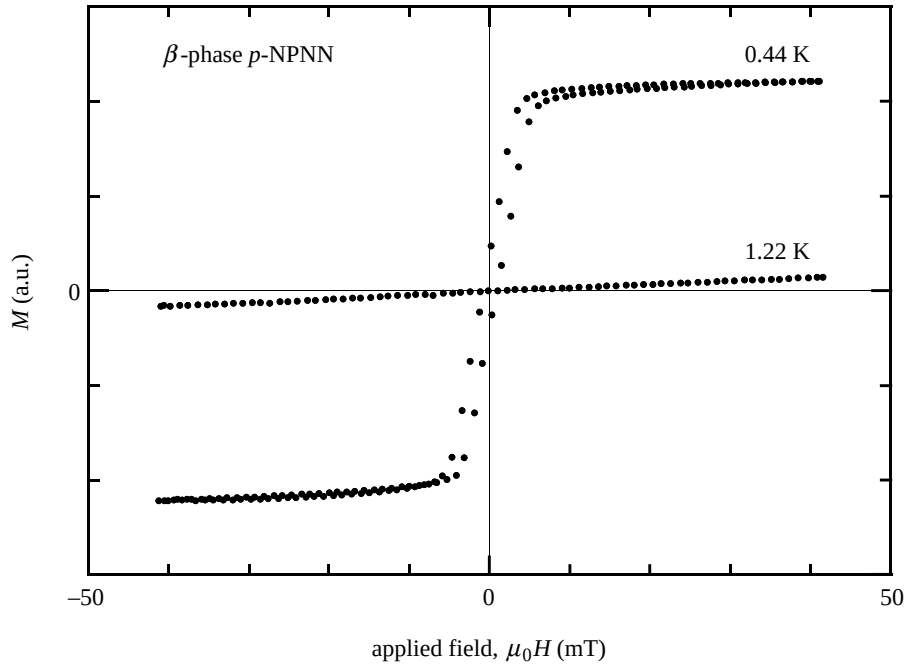

Figure 6. The magnetization curves of the β-phase p-NPNN measured at the temperatures above and below the transition temperature, T_c.

spin polarization is parallel to the b-axis. This suggests that the spin orientation in different domains is not aligned randomly and is most likely along the b-axis. Recent ferromagnetic resonance experiments (Oshima *et al.* 1995*a*, *b*) and neutron diffraction measurements by Schweizer's group (Zheludev *et al.* 1994*a*, *b*) also show that the magnetic easy axis is along the b-axis in the β-phase.

(*c*) *Neutron diffraction*

The spin density on each atom has been determined by neutron diffraction experiments (Zheludev *et al.* 1994*a*). This allows us to calculate the magnetic dipole–dipole interaction, $\boldsymbol{D}$, in the ordered state. According to our calculation, it is $D_a/k = -0.016$ K, $D_b/k = -0.029$ K and $D_c/k = +0.045$ K (Kinoshita 1994; see also Blundell *et al.* 1995). The spin system is most stable when the spin alignment is along the b-axis. This agrees with the easy axis assignment mentioned above.

(*d*) *Pressure effect*

When the pressure is applied to the crystal, the AC susceptibility exhibits remarkable changes. Figure 10 shows the pressure dependence of the AC susceptibility of the polycrystalline sample of β-phase p-NPNN up to $p = 1.04$ GPa measured under the AC field $H_{\mathrm{AC}}(\nu) < 1$ Oe ($= 10^3/4\pi$ A m^{-1}) with the frequency $\nu = 15.9$ Hz. It is found that the critical temperature, T_c, defined by the crossing point of the extrapolated lines from above and below T_c, approximately agrees with that determined from the heat capacity peak. As shown in figure 10, T_c shifts towards the

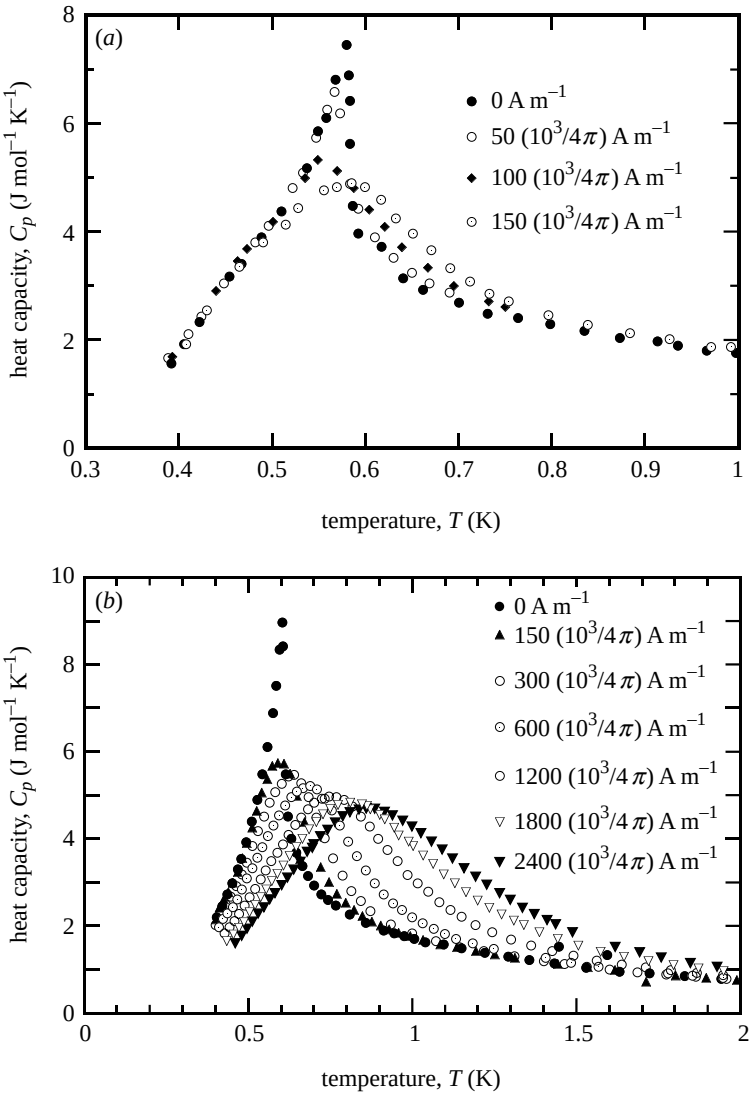

Figure 7. Temperature dependence of the heat capacity of the β-phase p-NPNN in the different applied magnetic field from 0 to 2400 Oe ($= 2400(10^3/4\pi)$ A m^{-1}).

lower temperature side with the initial gradient $\mathrm{d}[T_c(p)/T_c(p_0)]/\mathrm{d}p = -0.48\ \mathrm{GPa}^{-1}$, and the magnitude of the susceptibility decreases gradually as the pressure increases from p_0 ($= 0$ MPa). In the low-pressure region below $p \approx 650$ MPa, however, the ferromagnetic behaviour is still preserved below $T_c(p)$, as characterized by the shape of χ_{AC}.

In the high-pressure region above 650 MPa, on the contrary, the magnitude of χ_{AC} becomes quite small, the susceptibility in the ordered state decreases sensitively with the pressure increase, and the shoulder-like curve of χ_{AC} around $T_c(p)$ changes into a cusp, as shown in the inset of figure 10. Furthermore, $T_c(p)$ turns to increase as the pressure increases with a gradient of $\mathrm{d}[T_c(p)/T_c(p_c)]/\mathrm{d}p = +0.04\ \mathrm{GPa}^{-1}$, where

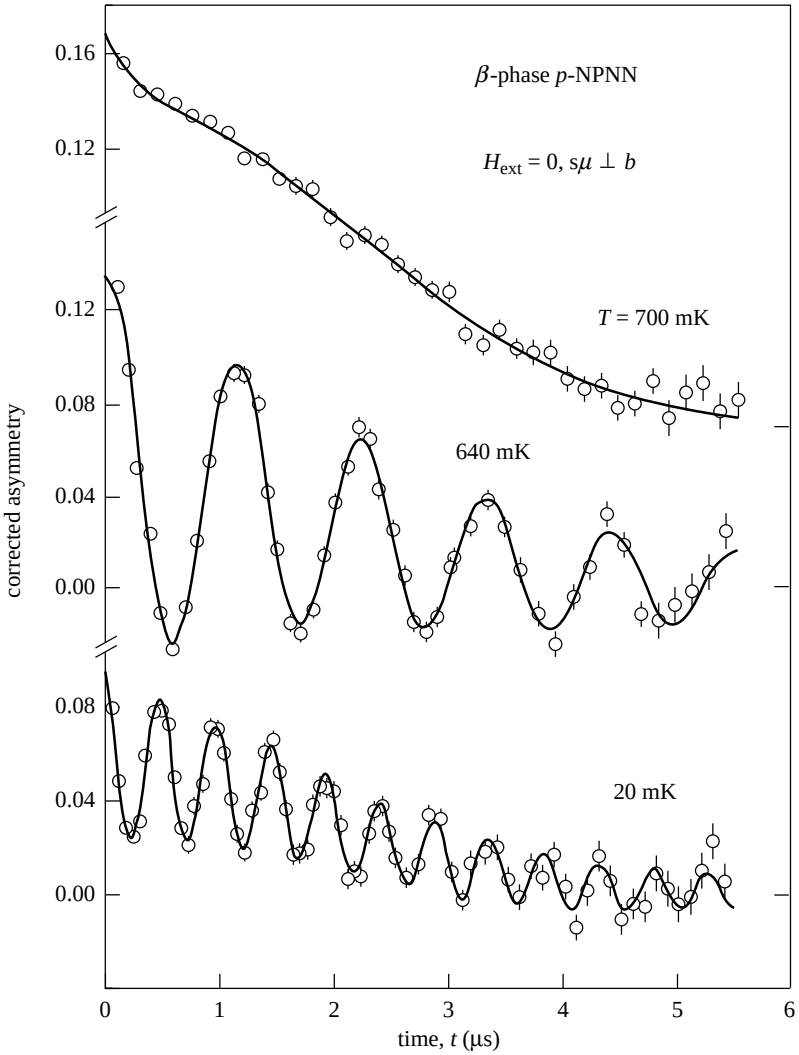

Figure 8. The ZF-μSR time spectra observed in the β-phase single crystals of p-NPNN with initial muon spin polarization perpendicular to the b-axis.

$p_c = 650 \pm 50$ MPa is the critical pressure. These results suggest that the magnetic order below T_c is of an antiferromagnet under high pressure.

The antiferromagnetic behaviour is also recognized in the external field dependence of χ_{AC} at constant pressure, $p = 690$ MPa, as shown in figure 11. $T_c(p)$ shifts to a lower temperature as the field increases, contrary to the case of a ferromagnet. Thus, we can conclude that pressurization induces a ferromagnetic-to-antiferromagnetic transition in the β-phase crystal.

7. Charge-transfer mechanism

These experimental results could be explained in terms of a charge-transfer mechanism by a competition between the ferromagnetic and antiferromagnetic interactions.

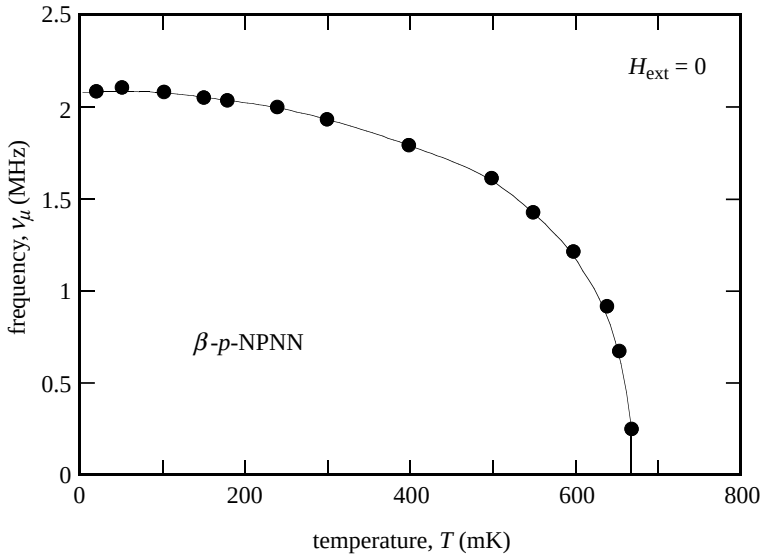

Figure 9. The temperature dependence of the muon spin precession frequency in the β-phase p-NPNN below T_c in a zero applied field. The frequency is proportional to the spontaneous magnetization, $M(T)$. The solid curve is a fit to the mean field magnetization $M(T) \propto [1-(T/T_c)^{\alpha}]^{\beta}$, with $\alpha = 1.86$ and $\beta = 0.32$.

The effective exchange interaction between molecules A and B contains the kinetic ($J^{\mathrm{K}}_{\mathrm{AB}}$) and the potential ($J^{\mathrm{P}}_{\mathrm{AB}}$) terms as

$$J_{\mathrm{AB}} = J^{\mathrm{K}}_{\mathrm{AB}} + J^{\mathrm{P}}_{\mathrm{AB}}. \tag{7.1}$$

Both terms depend on the overlap of molecular orbitals (MOs) on molecules A and B. The essential point of the charge-transfer mechanism is that the kinetic exchange interaction is described by a sum of terms contributing to antiferromagnetic and ferromagnetic interactions:

$$J^{\mathrm{K}}_{\mathrm{AB}} = -\frac{t^2_{\mathrm{SS}}}{U} + \frac{t^2_{\mathrm{SF}}}{U^2} J_{\mathrm{in}} + (\text{terms related to other paths}), \tag{7.2}$$

where t_{SS} denotes the transfer integral between the SOMOs of molecules A and B, t_{SF} the transfer integral between SOMO and other FOMOs, U is the on-site Coulomb repulsion, and J_{in} is the intramolecular exchange integral. Then interplay or frustration among these contributions may result in $J_{\mathrm{AB}} \approx 0$ for a certain condition, giving $T_c(p) \approx 0$ K. In the case of the β-phase of p-NPNN, we must take at least twelve interacting molecules adjacent to a central molecule in its zincblende-like structure of figure 2*b*. The corresponding exchange integrals are classified into three types, J_{12}, J_{13} and J_{14} (strictly speaking, J_{14} is further divided into two types) from the symmetry of the lattice. As mentioned before, J_{12} and J_{13} are, from theoretical calculation, known to be ferromagnetic and J_{14} is only weakly antiferromagnetic. On the other hand, reduction of the dimensionality from the three- to two-dimensional ferromagnetic system has been pointed out from the appearance of the short-range order effect by the heat capacity measurements under pressure (Takeda *et al*. 1995, 1996). From the crystal symmetry, it is obvious that only the exchange integral

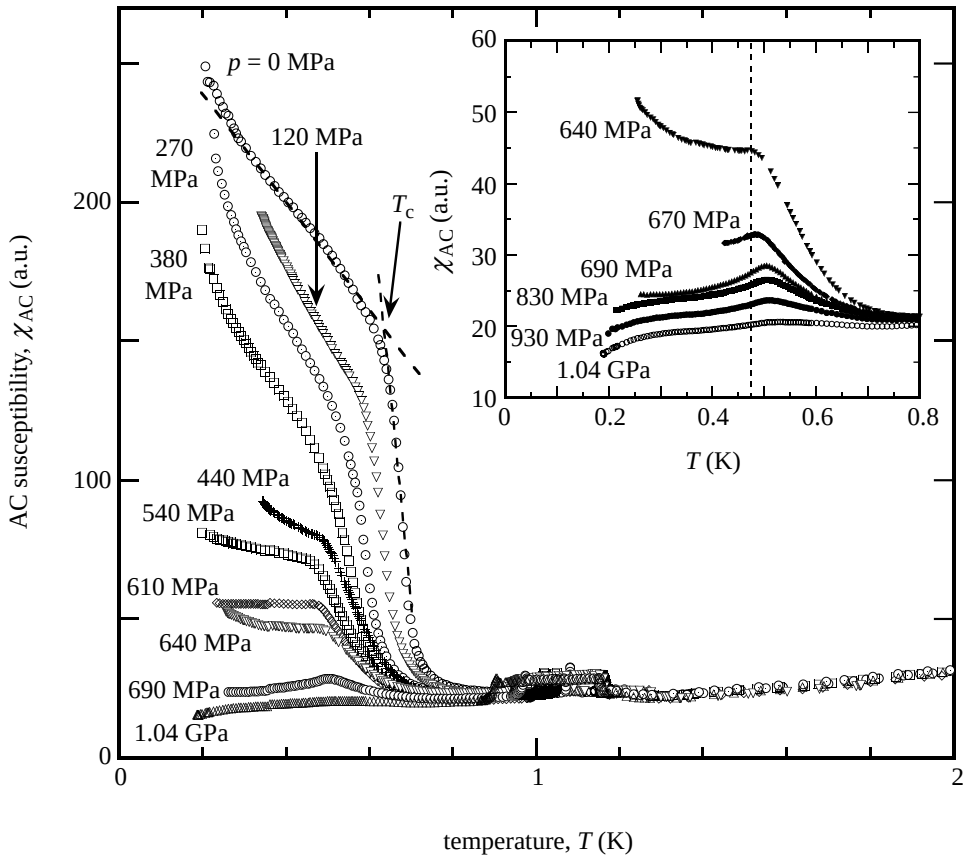

Figure 10. The temperature dependence of AC susceptibility of the polycrystalline β-phase p-NPNN under various pressures up to 1.04 GPa.

J_{12} is responsible for the two-dimensional ferromagnetic interaction. The transition temperature, T_{3D}, in such a reduced system can be written in terms of the mean field theory as

$$kT_{3D} \propto S^2\xi_{2D}^2(J_{12}, T_{3D})\{|J_{13} + J_{14}|\}, \tag{7.3}$$

where ξ_{2D} is the spin correlation length in the ac-plane in which $J_{12}/k \approx 0.8$ K is estimated from the heat capacity curve. Therefore, the antiferromagnetic behaviour at $p > p_c = 650 \pm 50$ MPa can be ascribed to a change in the sign of J_{13}. This means that the relative importance of the first and second terms in equation (7.2) relieve each other for J_{13} under high pressure.

8. Lattice constants under high pressure

The change of the magnetic interactions discussed above would be closely related to changes in molecular packing and deformation in the molecular shape. The lattice constants under various pressures have been determined by the Riedvelt method from the X-ray powder patterns obtained on the polycrystalline sample of β-phase p-NPNN by the use of imaging plates. The powder patterns observed are similar to

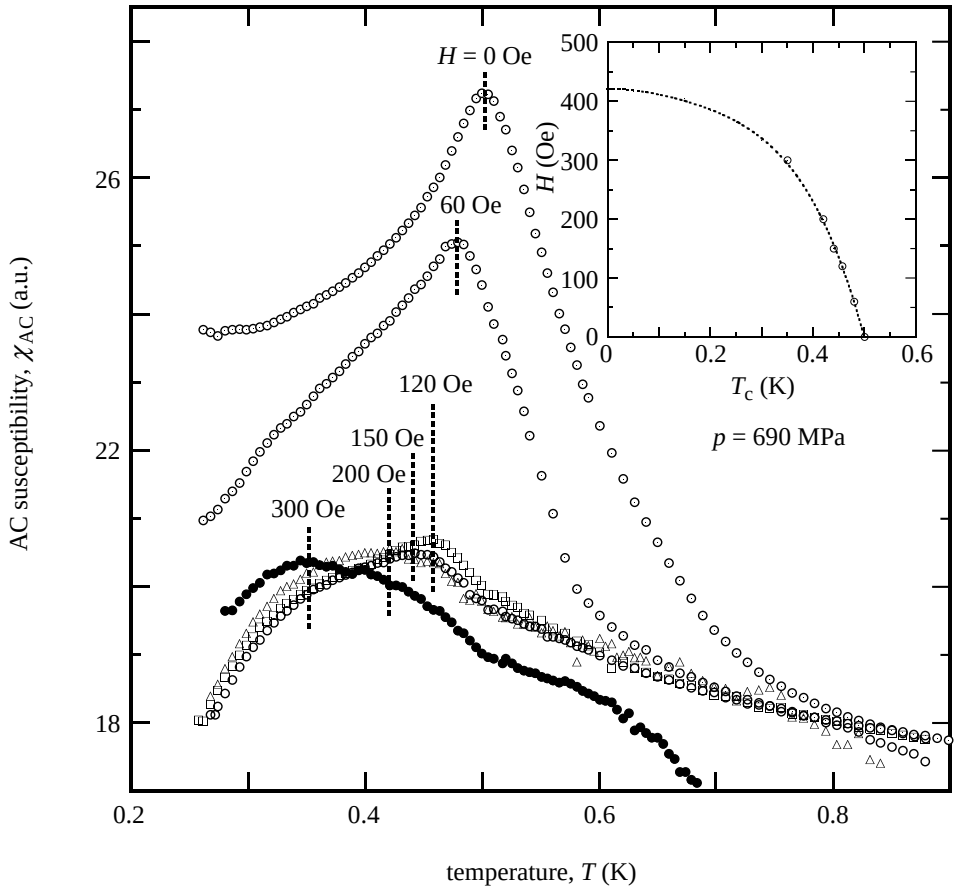

Figure 11. The temperature dependence of AC susceptibility of the β-phase p-NPNN at various external fields under the constant pressure of 690 MPa. The inset shows the T_c versus H phase boundary.

one another, indicating that the crystal symmetry is maintained under pressure up to 1.26 GPa (Takeda *et al*. 1998). The peak positions, of course, shift towards the direction of wider angles or to the direction of lattice contractions as the pressure increases. The lattice constants are plotted against pressure in figure 12. The crystal changes in two steps. The linear and volume compressibilities are summarized in table 2. The biggest contraction (*ca.* 4.5%) is found again along the *c*-axis as in the case of thermal contraction. The crystal density increases up to as large as 1.58 g cm^{-3} at 1.26 GPa.

The two-step contraction observed can be understood in the following way. The thermal contraction at 6 K nearly corresponds to the compressive contraction at *ca.* 400 MPa, although the thermal and compressive contraction of the lattice may or may not be the same. From this, we can expect that the molecules are librationally rotated about the *a*-axis to some extent more under pressures up to *ca.* 550 MPa. However, the plane of the nitro group is already in the upright orientation at 6 K (or at *ca.* 400 MPa) with respect to the *ac*-plane, and further pressurization beyond

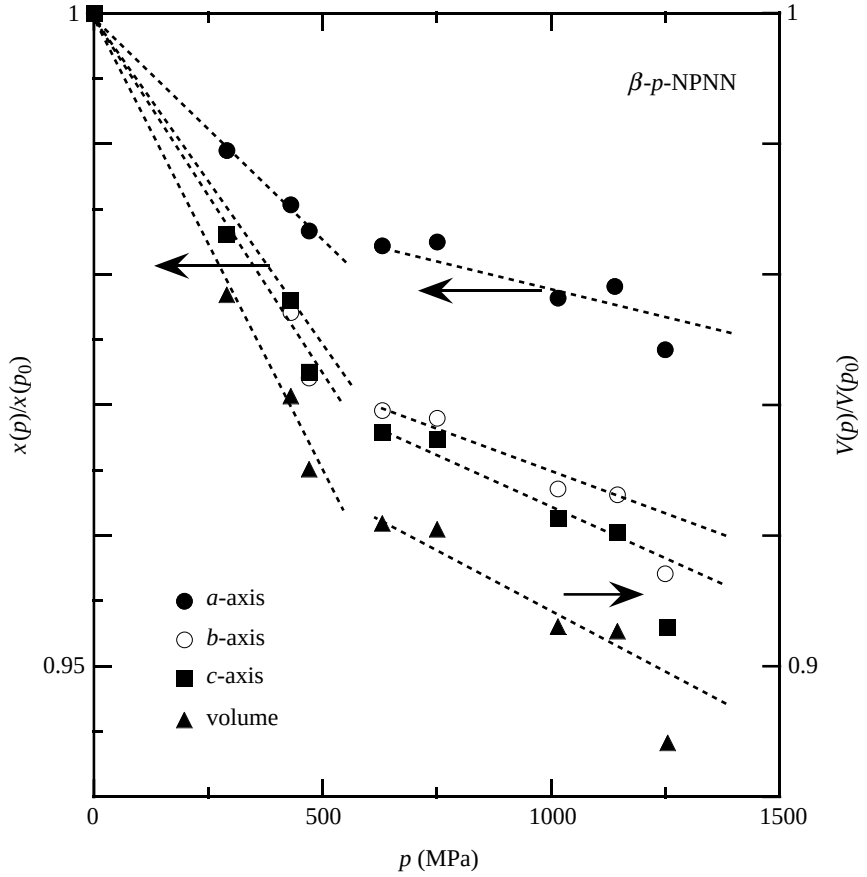

Figure 12. The pressure dependence of the lattice parameters and the unit-cell volume of the β-phase p-NPNN at room temperature.

Table 2. *Compressibility of the β-phase p-nitrophenyl nitronyl nitroxide crystal in units of* Pa^{-1}

	$\kappa_a = -\frac{1}{a}\frac{\partial a}{\partial p}$	$\kappa_b = -\frac{1}{b}\frac{\partial b}{\partial p}$	$\kappa_c = -\frac{1}{c}\frac{\partial c}{\partial p}$	$\kappa = -\frac{1}{V}\frac{\partial V}{\partial p}$
$p < 550$ MPa	34.4×10^{-11}	56.6×10^{-11}	55.1×10^{-11}	143×10^{-11}
$p > 550$ MPa	11.5×10^{-11}	18.4×10^{-11}	22.3×10^{-11}	49.0×10^{-11}

550 MPa will not increase the tilt angle further for the nitro group. Then, the other parts of the molecule can rotate internally about the long molecular axis under higher pressures. Internal rotations of the five-membered ring with the bulky tetramethylethylene group would be the most probable candidates to take place in order for the molecule to become more and more planar and for the crystal to become more compact.

Such molecular deformation would cause a change in the electronic structure of the molecule and in the intermolecular magnetic interactions. At this moment we cannot conclude definitely, because the crystal structure at very low temperature

and under high pressure is not available. However, it is natural to expect that the molecules take a more planar form and a more parallel arrangement in the crystal on compression at low temperature. The intermolecular charge-transfer interaction between the SOMOs on adjacent molecules would become more efficient, resulting in interchange of the importance of ferromagnetic and antiferromagnetic interactions, as discussed in the preceding section.

9. Other purely organic ferromagnets

Following the finding of the first example of an organic ferromagnet in the β-phase *p*-NPNN, a dozen of purely organic ferromagnets have been found. Some of them has been compiled in the literature (Kinoshita 1997). The highest ferromagnetic Curie temperature of 1.48 K was obtained for diazaadamantane dinitroxide (Chiarelli *et al*. 1993).

References

Allemand, P.-M., Fite, C., Canfield, P., Srdanov, G., Keder, N., Wudl, F. & Canfield, P. 1991 On the complexities of short range ferromagnetic exchange in a nitronyl nitroxide. *Synth. Met.* **41**–**43**, 3291–3295.

Awaga, K. & Maruyama, Y. 1989 Ferromagnetic intermolecular interaction of the organic radical, 2-(4-nitrophenyl)-4,4,5,5-tetramethyl-4,5-dihydro-1H-imidazolyl-1-oxyl 3-oxide. *Chem. Phys. Lett.* **158**, 556–558.

Awaga, K., Sugano, T. & Kinoshita, M. 1986*a* Organic radical clusters with ferromagnetic intermolecular interactions. *Solid State Commun.* **57**, 453–456.

Awaga, K., Sugano, T. & Kinoshita, M. 1986*b* Ferromagnetic intermolecular interactions in a series of organic mixed crystals of galvinoxyl radical and its precursory closed shell compound. *J. Chem. Phys.* **85**, 2211–2218.

Awaga, K., Sugano, T. & Kinoshita, M. 1986*c* ESR evidence for the ferro- and antiferro-magnetic intermolecular interaction in pure and dilute mixed crystals of galvinoxyl. *Chem. Phys. Lett.* **128**, 587–590.

Awaga, K., Sugano, T. & Kinoshita, M. 1987*a* Thermodynamic properties of the mixed crystals of galvinoxyl radical and its precursory closed shell compound: the large entropy cooperating with the spin system. *J. Chem. Phys.* **87**, 3062–3068.

Awaga, K., Sugano, T. & Kinoshita, M. 1987*b* Ferromagnetic intermolecular interaction of the galvinoxyl radical: cooperation of spin polarization and charge-transfer interaction. *Chem. Phys. Lett.* **141**, 540–544.

Awaga, K., Sugano, T. & Kinoshita, M. 1988 Ferromagnetic intermolecular interaction of organic radical, galvinoxyl. *Synth. Met.* **27**, B631–B638.

Awaga, K., Inabe, T., Nagashima, U. & Maruyama, Y. 1989*a* Two-dimensional network of the ferromagnetic radical, 2-(4-nitrophenyl)-4,4,5,5-tetramethyl-4,5-dihydro-1H-imidazol-1-oxyl 3-N-oxide. *J. Chem. Soc. Chem. Commun.*, pp. 1617–1618.

Blundell, S. J., Pattenden, P. A., Pratt, F. L., Valladares, R. M., Sugano, T. & Hayes, W. 1995 μ^+SR of the organic ferromagnet *p*-NPNN: diamagnetic and paramagnetic states. *Europhys. Lett.* **31**, 573–578.

Chiarelli, R., Novak, M. A., Rassat, A. & Tholence, J. L. 1993 A ferromagnetic transition at 1.48 K in an organic nitroxide. *Nature* **363**, 147–149.

Hosokoshi, Y., Tamura, M. & Kinoshita, M. 1997 Pressure effect on organic radicals. *Mol. Cryst. Liq. Cryst.* **306**, 423–430.

Kinoshita, M. 1991 Intermolecular ferromagnetic coupling in organic radical crystals. In *Magnetic molecular materials* (ed. D. Gatteschi, O. Kahn, J. S. Miller & F. Palacio). NATO ASI Series E, vol. 198, pp. 87–103.

Kinoshita, M. 1993*a* Ferromagnetism in organic radical crystal. *Mol. Cryst. Liq. Cryst.* **232**, 1–12.

Kinoshita, M. 1993*b* Bulk ferromagnetism of the crystal of the organic radical, *p*-NPNN. *Synth. Met.* **56**, 3279–3284.

Kinoshita, M. 1994 Ferromagnetism of organic radical crystals. *Jap. J. Appl. Phys.* **33**, 5718–5733.

Kinoshita, M. 1995 Ferromagnetism and antiferromagnetism in organic radical crystals. *Physica* B **213/214**, 257–261.

Kinoshita, M. 1996 Organic magnetic materials with cooperative magnetic properties. In *Molecular magnetism. From molecular assemblies to the devices* (ed. P. Coronado, D. Delhaes, D. Gatteschi & J. S. Miller). NATO ASI Series E, vol. 321, pp. 449–472.

Kinoshita, M. 1997 Magnetic properties of organic solids. In *Organic molecular solids. Properties and applications* (ed. W. Jones), pp. 379–414. Boca Raton, FL: CRC.

Le, L. P., Keren, A., Luke, G. M., Wu, W. D., Uemura, Y. J., Tamura, M., Ishikawa, M. & Kinoshita, M. 1993 Searching for spontaneous magnetic order in an organic ferromagnet. μSR studies of β-phase *p*-NPNN. *Chem. Phys. Lett.* **206**, 405–408.

McConnell, H. M. 1963 Ferromagnetism in solid free radicals. *J. Chem. Phys.* **39**, 1910.

Mito, M., Kawae, T., Takumi, M., Nagata, K., Tamura, M., Kinoshita, M. & Takeda, K. 1997 Pressure-induced ferro- to antiferromagnetic transition in a purely organic compound, β-phase *p*-nitrophenyl nitronyl nitroxide. *Phys. Rev.* B **56**, 14 255–14 258.

Mukai, K. 1969 Anomalous magnetic properties of stable crystalline phenoxyl radicals. *Bull. Chem. Soc. Jap.* **42**, 40–46.

Mukai, K., Nishiguchi, H. & Deguchi, Y. 1967 Anomaly in the χ–T curve of galvinoxyl radical. *J. Phys. Soc. Jap.* **23**, 125.

Nakazawa, Y., Tamura, M., Shirakawa, N., Shiomi, D., Takahashi, M., Kinoshita, M. & Ishikawa, M. 1992 Low-temperature magnetic properties of ferromagnetic organic radical, *p*-nitrophenyl nitronyl nitroxide. *Phys. Rev.* B **46**, 8906–8914.

Okumura, M., Mori, W. & Yamaguchi, K. 1993 *Mol. Cryst. Liq. Cryst.* **232**, 35–44.

Oshima, K., Kawanoue, H., Haibara, Y., Yamazaki, H., Awaga, K., Tamura, M., Ishikawa, M. & Kinoshita, M. 1995*a* Ferromagnetic resonance and nonlinear absorption in *p*-NPNN. *Synth. Met.* **71**, 1821–1822.

Oshima, H., Haibara, Y., Yamazaki, H., Awaga, K., Tamura, M. & Kinoshita, M. 1995*b* Ferromagnetic resonance in *p*-NPNN below 1 K. *Mol. Cryst. Liq. Cryst.* **271**, 29–34.

Takeda, K., Konishi, K., Tamura, M. & Kinoshita, M. 1995 Magnetism of the β-phase *p*-nitrophenyl nitronyl nitroxide crystal. *Mol. Cryst. Liq. Cryst.* **273**, 57–66.

Takeda, K., Konishi, K., Tamura, M. & Kinoshita, M. 1996 Pressure effects on intermolecular interactions of the organic ferromagnetic crystalline β-phase *p*-nitrophenyl nitronyl nitroxide. *Phys. Rev.* B **53**, 3374–3380.

Takeda, K., Mito, M., Kawae, T., Takumi, M., Nagata, K., Tamura, M. & Kinoshita, M. 1998 Pressure dependence of intermolecular interactions in the genuine organic β-phase *p*-nitrophenyl nitronyl nitroxide crystal accompanying a ferro- to antiferromagnetic transition. *J. Phys. Chem.* B **102**, 671–676.

Tamura, M., Nakazawa, Y., Shiomi, D., Nozawa, K., Hosokoshi, Y., Ishikawa, M., Takahashi, M. & Kinoshita, M. 1991 Bulk ferromagnetism in the β-phase crystal of the *p*-nitrophenyl nitronyl nitroxide radical. *Chem. Phys. Lett.* **186**, 401–404.

Turek, P., Nozawa, K., Shiomi, D., Awaga, K., Inabe, T., Maruyama, Y. & Kinoshita, M. 1991 Ferromagnetic coupling in a new phase of the *p*-nitrophenyl nitronyl nitroxide radical. *Chem. Phys. Lett.* **180**, 327–331.

Uemura, Y. J., Le, L. P. & Luke, G. M. 1993 Muon spin relaxation studies in organic superconductors and organic magnets. *Synth. Met.* **56**, 2845–2850.

Zheludev, A., Ressouche, M. & Schweizer, E. 1994*a* Neutron diffraction of a ferromagnetic phase transition in a purely organic crystal. *Solid State Commun.* **90**, 233–235.

Zheludev, A., Bonnet, M., Ressouche, E., Schweizer, J., Wan, M. & Wang, H. 1994*b* Experimental spin density in the first purely organic ferromagnet: the β-para-nitrophenyl nitronyl nitroxide. *J. Mag. Mag. Mater.* **135**, 147–160.

Discussion

P. Day (*The Royal Institution, London, UK*). In view of the large size of the crystals of NPNN that are available, have any coherent inelastic neutron scattering experiments been carried out to define the spin wave dispersion along the various crystallographic directions? I ask because the crystal structure suggests that the magnetic correlations may be quite strongly two dimensional in character.

M. Kinoshita. No, we have not done such experiments. However, the dominant two-dimensional character of this compound was suggested from heat capacity analysis. The temperature dependence of the magnetic heat capacity is well explained theoretically by introducing a small correction to a square lattice model.